ELSEVIER

Journal of Hydrology 164 (1995) 89–107

Journal of Hydrology

[1]

Fluxes of water and solute in a coastal wetland sediment. 1. The contribution of regional groundwater discharge

William K. Nuttle[a], Judson W. Harvey[b,*]

[a]*11 Craig Street, Ottawa, Ont., Canada K1S 4B6*

[b]*Water Resources Division, US Geological Survey, 345 Middlefield Road, Mail Stop 496, Menlo Park, CA 94025, USA*

Received 16 December 1993; revision accepted 22 June 1994

Abstract

Upward discharge of fresh groundwater into a mid-Atlantic intertidal wetland contributed 62% of the water needed to replace evapotranspiration losses from the sediment during an 11 day period in September. Infiltration during flooding by tides provided most of the balance; thus there was a net advection of salt into the sediment. The amount of groundwater discharge was estimated from changes in water storage in the sediment, as inferred from measurements of hydraulic head made every 10 min. We argue that this approach is inherently more accurate than calculating the flux as the product of hydraulic conductivity and head gradient. Evapotranspiration was estimated from direct measurements of net radiation. On an annual time-scale, our results suggest that groundwater discharge at this site may exceed the evapotranspiration flux during months of reduced evapotranspiration. Should this occur, groundwater-driven advection would supplement diffusion, during flooding, in removing salt from the sediment.

1. Introduction

Groundwater discharge into the coastal zone influences the structure and productivity of nearshore ecosystems by providing localized sources of nutrients and areas of reduced salinity (Johannes, 1980; Johannes and Hearn, 1985; Capone and Slater, 1990). The latter may be especially important in intertidal coastal wetlands where high evapotranspiration rates and recharge by brackish water favor the accumulation of salt in the sediment. Evapotranspiration is the dominant mechanism for removing water from these wetland sediments (Yelverton and

* Corresponding author.

Elsevier Science B.V.
SSDI 0022-1694(94)02561-O

Hackney, 1986; Harvey et al., 1987; Nuttle and Hemond, 1988). The sediment is resaturated each time the wetlands are inundated at high tide. Subsequent removal of porewater by evapotranspiration leaves salt behind, resulting in a net advective flux of salt into the sediment (Nuttle and Hemond, 1988). It has been suggested that the efficiency of salt removal from the sediment influences primary production in these highly productive ecosystems (Morris et al., 1990).

Intertidal wetlands occupy areas of general upward groundwater flow driven by discharge from the regional groundwater flow system (Reilly and Goodman, 1985; Harvey and Odum, 1990). Where the influx of fresh groundwater into intertidal wetland sediments from below is sufficiently large, it provides an alternative to tidal water as a source of water to balance evapotranspiration losses, thus limiting advection of salt into the sediment. Also, during the time of the year when evapotranspiration is low the influx of fresh groundwater may exceed water loss by evapotranspiration, leading to the situation in which groundwater drives a net upward flow of water and salt out across the sediment surface. In this paper, we estimate the groundwater flux by reconstructing the sediment water balance at a site in an intertidal wetland for a period of 11 days, and we examine the role of groundwater in controlling the advection of salt into the sediment. Factors contributing to the removal of salt by diffusion are the subject of a companion paper (Harvey and Nuttle, 1995).

Groundwater flow into the sediment was estimated as one parameter in a transient water balance model fitted to measurements of hydraulic head. The model accounts for the response of head to transient water fluxes across the sediment surface and the inflow of groundwater from below. This approach borrows from the combined transient flow and water budget (TFWB) method developed for monitoring water use in agricultural crops. Recently, the TFWB method has been applied to estimate aquifer recharge by water from the vadose zone (Schuh et al., 1993a,b). The TFWB method uses measurements of the changes in soil moisture potential over time at several depths. These are combined with in-situ measurements of soil hydraulic properties to estimate evapotranspiration and groundwater recharge fluxes. In contrast, the analysis applied in this study uses observations of hydraulic head (including tension head) in the upper layer of the sediment and independent estimates of the evapotranspiration flux to estimate the sediment hydraulic parameters and the flux of groundwater into the sediment.

Methods for estimating the values for parameters in groundwater models from measured hydraulic head and recharge fluxes are the subject of a large body of research (e.g. Yeh, 1986; Keidser and Rosbjerg, 1991). Parameter estimation for groundwater models is complicated by spatial variability in hydraulic properties of aquifers, which has the effect of increasing the potential number of model parameters. And typically, observations of head are available at only a few, sparsely distributed locations in a multi-dimensional model domain. The water balance model used here is a zero-dimensional, lumped parameter model containing at most three unknown parameters. As a consequence of this simplicity we are able to estimate values for the model parameters through direct application of standard non-linear regression techniques.

1.1. Formulation of the sediment water balance

Changes in hydraulic head in a discrete volume of sediment are directly related to changes in the amount of water it contains. Following the formulation of the water budget for an intertidal wetland in Nuttle and Hemond (1988), this relationship can be stated as

$$V_B S_S \frac{dh}{dt} = \oint_{V_B} -(\boldsymbol{q}_S + \boldsymbol{q}_v + \boldsymbol{q}_h)d\boldsymbol{s} \tag{1}$$

in which h is the hydraulic head (cm), V_B is the volume over which h is defined (cm^3), S_S is specific storage of the sediment (cm^{-1}), $\boldsymbol{q}_S$ is net water flux across the sediment surface (cm s^{-1}), $\boldsymbol{q}_v$ is vertical flow to an underlying aquifer (cm s^{-1}), $\boldsymbol{q}_h$ is horizontal flux within the wetland sediment (cm s^{-1}), and $d\boldsymbol{s}$ is the differential surface area (cm^2). The bold type denotes vector quantities. Net water flux across the sediment surface is the difference of evapotranspiration and infiltration.

The sediment water budget can be recast in terms of the net water fluxes per unit (horizontal) area of marsh (Fig. 1). Horizontal fluxes within the sediment are a significant component of the water budget in intertidal wetlands only within a few meters of a creek bank (Nuttle and Hemond, 1988). Our study site is far from creek banks and any other feature with large vertical relief; therefore we assume $q_h = 0$. By applying Darcy's law, one can express q_v as the product of vertical hydraulic conductivity and hydraulic head gradient along the path between the sediment and the underlying aquifer

$$\frac{dh}{dt} = \frac{q_S}{S_y} + \frac{K_v}{S_y D}(h_a - h) + \epsilon_m \tag{2}$$

in which S_y is specific yield (cm cm^{-1}), K_v is vertical hydraulic conductivity (cm s^{-1}), h_a is hydraulic head in the underlying aquifer (cm), D is depth to the point at which h_a is defined (cm), and ϵ_m is model error introduced by the assumptions above. It should

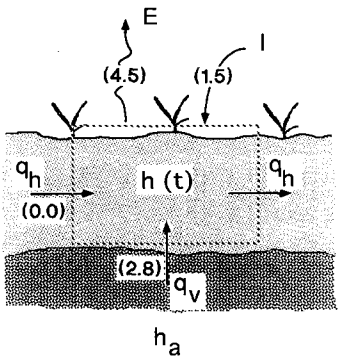

Fig. 1. Water balance in the sediment showing evapotranspiration (E), infiltration (I), horizontal fluxes within the sediment (q_h), and groundwater discharging into the sediment (q_v) from an underlying aquifer. Values are averages (mm day^{-1}) for the 11 day period.

be noted that water fluxes at the surface are considered positive when directed into the sediment.

1.2. General model for changes in observed head

Eq. (2) is the basis for estimating short-term water fluxes from a series of hydraulic head measurements. Interpretation of measured head must also account for the presence of measurement error, especially in the work described below where this error may be comparable in magnitude with changes in head caused by the water fluxes that are to be estimated. Measurement error is the difference between 'observed' head and the real head, and there are two components of this error, systematic error and random error;

$$h^* = h + \epsilon_s + \epsilon_r \tag{3}$$

in which h^* is observed head, ϵ_s is systematic error, and ϵ_r is random error.

Systematic error is caused by confounding factors in the measurement process that introduce a bias into the measurements and can be considered to be a function of these factors. In principle, systematic error can be estimated and removed from measurements if a thorough calibration of the measuring instrument is performed. In contrast, random error is the irreducible imprecision inherent in the measurement, and it is often represented as a random variable with mean value equal to zero.

For example, let us consider a systematic error caused by the effect of ambient temperature on an instrument for measuring hydraulic head. In the general case, the systematic error is a function of both temperature, θ, and head; $\epsilon_s = f(\theta, h)$. The contribution of systematic error in an incremental change in observed head is defined by

$$\begin{aligned} dh^* &= dh + \frac{\partial \epsilon_s}{\partial h} dh + \frac{\partial \epsilon_s}{\partial \theta} d\theta + d\epsilon_r \\ &= \left[1 + \frac{\partial \epsilon_s}{\partial h}\right] dh + \frac{\partial \epsilon_s}{\partial \theta} d\theta + d\epsilon_r \end{aligned} \tag{4}$$

Combining the equation above with the water balance equation, Eq. (2), and integrating over the time period $t_1 < t < t_2$, we obtain a general model for interpreting changes in observed head over time;

$$\Delta h^* = \int_{t_1}^{t_2} \frac{dh^*}{dt} dt = \underset{(1)}{\left[1 + \overline{\frac{\partial \epsilon_s}{\partial h}}\right]} \underset{(2)}{\left[\frac{1}{S_y} \int_{t_1}^{t_2} q_s dt + \frac{K_v}{S_y D} h_a (t_2 - t_1) - \frac{K_v}{S_y D} \int_{t_1}^{t_2} h dt\right]}$$

$$\underset{(3)}{+ \overline{\frac{\partial \epsilon_s}{\partial \theta}}} \underset{(4)}{(\theta_2 - \theta_1)} + \underset{(5)}{\Delta \epsilon_r + \epsilon_m} \tag{5}$$

in which Δh^* is change in observed head, $\overline{\partial \epsilon_s / \partial h}$ and $\overline{\partial \epsilon_s / \partial \theta}$ are the averages for the

period; θ_1 and θ_2 are temperature at t_1 and t_2, respectively; $\Delta\epsilon_r$ is random error in Δh^*, and the other variables are as defined above, except the model error, ϵ_m, which differs from that in Eq. (2). The numbered terms on the right-hand side of Eq. (5) are (1) a systematic error term, multiplying the sum of contributions due to (2) evapotranspiration, (3) constant groundwater recharge, and (4) head-dependent groundwater recharge, and (5) another systematic error term. $\Delta\epsilon_r$ is the difference between two random variables each distributed as ϵ_r; therefore the variance of $\Delta\epsilon_r$ is twice the variance of ϵ_r.

Below we use the term 'residual error' to refer to the sum $\Delta\epsilon_r + \epsilon_m$ in Eq. (5), that is, the difference between the change in observed head and that calculated using a water balance model. Our objective is to identify a particular model, and estimate its parameters, so as to minimize the residual error. In this we can affect only the portion of the residual error contributed by model error; the systematic error, ϵ_s, is explicitly included in the model. Random error in observed head does not change, given a set of data. Thus the random error sets a limit on how much the residual error can be reduced by improvements in the model.

2. Methods

2.1. Study site

The study site is part of the Virginia Coast Reserve Long Term Ecological Research site, near Nasawadox, Virginia, on the Atlantic Ocean side of the Delmarva Peninsula (37°27′N, 75°50′W) (Fig. 2). The wetland is set in the Bell Neck complex (Mixon, 1985), which is made up of a mosaic of agricultural and forested upland, freshwater and intertidal wetlands and tidal creeks.

The Bell Neck complex is bounded on the east by a coastal lagoon–barrier island complex and on the west by older, higher marine deposits that form the spine of the Delmarva peninsula. At least six low-lying (less than 3 m above mean sea-level) relic beach ridges can be identified from topographic maps, running parallel to the coast in the vicinity of the study site. The ridges are cut through by tidal creeks, and the area between the ridges is overlain by a veneer of intertidal sediments, mud flats and salt marshes. Water balance measurements were performed at a site on the axis of one of these ridges, in a wetland drained by Phillips Creek. The wetland sediments at the study site consist of a layer of organic-rich, estuarine clays about 2 m thick. A more detailed description of the sediments has been given by Harvey and Nuttle (1995).

The Wachapreague formation (Mixon, 1985) lies beneath the Bell Neck complex at the study site and serves as the unconfined aquifer in the relic beach ridges. This deposit consists of approximately 12 m of sand, silt and clay. Water from the Yorktown aquifer discharges into the unconfined groundwater system in the Wachapreague formation at the study site. The Yorktown aquifer (approximately 45 m thick) underlies the Wachapreague formation and extends westward beneath the entire Delmarva Peninsula and the Chesapeake Bay. In the ridge immediately north of the study site, the annual mean piezometric head in the Yorktown aquifer stands

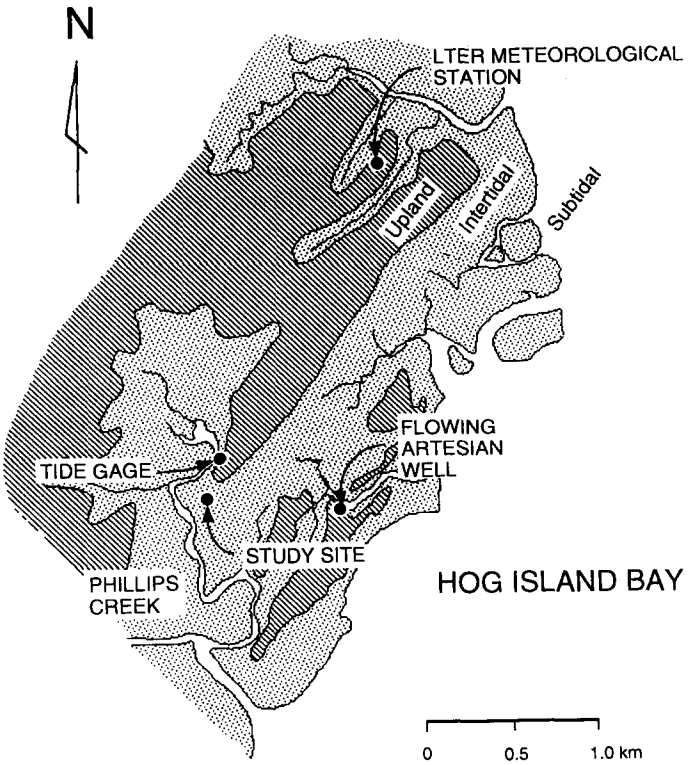

Fig. 2. Study site located within the Virginia Coast Reserve Long Term Ecological Research site on Virginia's Atlantic coast.

about 1 m above the annual mean water table, and a net inflow of groundwater was required to close the annual water budget in the unconfined aquifer in 1989 (Fetsko, 1990). Artesian conditions in the Yorktown aquifer extend east of the study site at least to the next relic beach ridge (0.5 km away) where a flowing artesian well discharges at the elevation of mean high water.

2.2. Observed hydraulic head

Instantaneous measurements of hydraulic head were recorded at 10 min intervals over 11 days (27 August–7 September 1989) using pressure transducer tensiometers and an electronic datalogger. Measurements were made at 10 and 20 cm below the surface and averaged, so observed head can be taken as the average hydraulic head in the upper 30 cm or so of sediment. The pressure transducer tensiometers were constructed of pressure transducers connected via a small gas head space to a water-filled polycarbonate tube fitted with a porous ceramic cup and inserted into the sediment. Details of the construction of the pressure transducers and of problems encountered with their calibration have been given by Hoelscher et al. (1993).

Tensiometers were used, rather than simpler piezometers, because we originally hoped to observe vertical head gradients in conjunction with evapotranspiration and infiltration, and we anticipated that negative (gage) pore pressures would occur during periods of evapotranspiration at the shallow depths that we were monitoring. The tensiometers were designed to measure pressure heads in the range +100 cm to −100 cm, which bounds the expected range of head in shallow sediments defined by flooded conditions with water ponded on the surface and relatively dry conditions after a few days without flooding or precipitation. Even when 'dry' the water table in intertidal wetlands is typically within 30 cm of the surface.

2.3. Evapotranspiration and infiltration

Conditions related to evapotranspiration and infiltration fluxes at the sediment surface were also observed at the site. Creek water levels were recorded continuously by a tide gage in the closest tidal creek to the site, 300 m away. Periods of surface flooding were identified from this record as periods when the water level in the creek was above the elevation of the sediment surface. Evapotranspiration was calculated from net radiation measured at 10 min intervals using a Fritschen-type transducer mounted 3 m above the sediment surface. Air temperature was also measured at 10 min intervals using a shielded thermistor mounted 2 m above the surface. Hourly summaries of wind speed and direction and precipitation were available for an automated weather station 2 km from the site.

Estimated evapotranspiration was calculated from measured net radiation using the Priestly–Taylor formula for daytime potential evapotranspiration under moist conditions (Priestly and Taylor, 1972). We assumed that no evapotranspiration occurred at night and that evapotranspiration was not limited by the availability of water during the daylight hours. The Priestly–Taylor formula has been found to work well in estimating the evapotranspiration flux in water balance studies in other intertidal wetlands (Nuttle and Hemond, 1988; Price and Woo, 1988). Perhaps the largest source of error in estimating evapotranspiration is in the measurement of net radiation. We estimate that the error in evapotranspiration calculated as described above can be as high as 20%, conservatively based on intercomparisons among a number of net radiation sensors by Field et al. (1992).

2.4. Statistical analysis

The record of observed head was analyzed in two stages. The first stage of analysis consisted of identifying and estimating parameter values for the best water balance model. The best model was selected from a set of six candidate models (Table 1) each derived from the general model for the change in observed head over discrete time intervals (Eq. (5)). The six candidate models represent three hypotheses about the nature of the water balance (during non-flooding periods): (1) variable evapotranspiration is the only water flux during non-flooding periods; (2) variable evapotranspiration and constant recharge from the aquifer are the principal fluxes; (3) variable evapotranspiration and head-dependent recharge are the fluxes during

Table 1
Fluxes included in the water balance models

Flux	Models 1a, 1b	Models 2a, 2b	Models 3a, 3b
Evapotranspiration	XXX	XXX	XXX
Constant groundwater flux		XXX	XXX
Head-dependent groundwater flux			XXX

non-flooding periods. Each of these models was considered excluding (Models 1a, 2a and 3a) or including (Models 1b, 2b and 3b) a systematic error in observed head having the form

$$\epsilon_s = \frac{A}{B}(\theta - \theta_r)(h - h_r) \tag{6}$$

in which h is hydraulic head, θ is ambient temperature, and A, B, θ_r, and h_r are calibration constants. (Refer to the Appendix for the derivation of this error term.)

The 11 day period of data collection was divided into time intervals based on water fluxes across the sediment surface. Three types of intervals were defined; (1) flooding periods with the surface flux dominated by infiltration; (2) non-flooding, evapotranspiration periods with the surface flux equal to evapotranspiration; (3) non-flooding, night-time periods when the surface flux was assumed to be zero. (Infiltration occurred only during tidal flooding as no precipitation fell during the period of measurement.) These intervals defined the data used to estimate the model parameters by non-linear regression analysis.

For the sake of simplicity in the model identification stage we assumed that the model parameters are constant. Of course, the hydraulic properties of the sediment are affected by changes in the water content, for which changes in observed head can be used as a proxy measure. Hydraulic conductivity can change by orders of magnitude in the first stages of desaturation owing to the loss of the conductance of the largest pores. However, the water balance models used here are relatively insensitive to these changes. Hydraulic conductivity is used in the models to parametrize the flow between the underlying aquifer and bottom of the upper 30 cm or so of sediment. This pathway is always saturated except in cases of extreme drawdown of the water table. Specific yield also changes as the water table in the sediment rises and falls within 30 cm of the surface, but the changes are less pronounced than those of hydraulic conductivity (Nuttle, 1988).

We controlled for the effect of variation in hydraulic properties by evaluating the sensitivity of the estimated parameter values to changes in head (water content) in the second stage of analysis. The time-interval data were subdivided into four sets based on the mean observed head during the period ($10 < h < 20$; $0 < h < 10$; $-10 < h < 0$; $-20 < h < -10$). Then the parameters of the best model were re-estimated by regression for each subset of data.

Periods of flooding and infiltration into the sediment were excluded from the analysis for two reasons. First, there was no way of independently estimating the surface flux during infiltration. Second, inferring the change in water storage from the response of observed head during these periods is complicated by the effect on pore pressures of static loading of the sediment by the water flooding the surface, and this is not accounted for in Eq. (5) (Hemond et al., 1984). Therefore the value of the additional information contained in these data was offset by the increase in the complexity of the water balance model, including the addition of unknown parameters, which would have been required to include these data in our analysis.

Non-linear least-squares analysis (Draper and Smith, 1981) was used to estimate the model parameters and calculate the errors in these estimates and the residual error. The analysis was conducted using the NLIN procedure in the SAS statistical package (Statistical Analysis Systems Institute, Inc., 1989). In performing the analysis, the change in observed head during each period was the dependent variable; the parameters to be estimated for each model are specified in Table 2; and the independent variables obtained from data measured in the field for each period were the following: EVAP, wet potential evapotranspiration ($\text{EVAP} \approx \int_{t_1}^{t_2} q_s \mathrm{d}t$); Δt, length of time period $(t_2 - t_1)$; $\bar{h} = \frac{1}{2}(h_2^* + h_1^*) \approx [1/(t_2 - t_1)] \int_{t_1}^{t_2} h \mathrm{d}t$; $\text{TEMP} = \frac{1}{2}(\theta_2 + \theta_1) - \theta_r$, where θ_r is 25°C; $\Delta\text{TEMP} = \theta_2 - \theta_1$; $\overline{\partial \epsilon_s / \partial h} = A/B$ TEMP; $\overline{\partial \epsilon_s / \partial \theta} = A/B(\bar{h} - h_r)$, where h_r is 1.35 cm.

Table 2
Summary of equations used in non-linear regression

Model 1a: Evapotranspiration only;

$\Delta h^* = C_1 \text{EVAP}$

Model 2a: Evapotranspiration with constant groundwater flow;

$\Delta h^* = (C_1 \text{EVAP}) + (C_2 \Delta t)$

Model 3a: Evapotranspiration, constant groundwater flow and head-dependent recharge;

$\Delta h^* = (C_1 \text{EVAP}) + (C_3 \Delta t) + (C_4 \bar{h} \Delta t)$

Model 1b: same as 1a with temperature effect;

$\Delta h^* = (1 + C_5 \text{TEMP})(C_1 \text{EVAP}) + C_5(\bar{h} - h_r)\Delta\text{TEMP}$

Model 2b: same as 2a with temperature effect;

$\Delta h^* = (1 + C_5 \text{TEMP})[(C_1 \text{EVAP}) + (C_2 \Delta +)] + C_5(\bar{h} - h_r)\Delta\text{TEMP}$

Model 3b: same as 3a with temperature effect;

$\Delta h^* = (1 + C_5 \text{TEMP})[(C_1 \text{EVAP}) + (C_3 \Delta +) + (C_4 \bar{h} \Delta t)] + C_5(\bar{h} - h_r)\Delta\text{TEMP}$

Physical meaning of regression coefficients: $C_1 = -1/S_y$ (cm mm^{-1}); $C_2 = K_v(h_a - \langle h \rangle)/S_y D$ (cm day^{-1}), where $\langle h \rangle$ is the head in sediment averaged over the entire 11 day period; $C_3 = K_v h_a / S_y D$ (cm day^{-1}); $C_4 = -K_v / S_y D$ (day^{-1}); $C_5 = A/B$ (see Appendix).

3. Results

Continuous records of hydraulic head in the sediment, tide height, and evapotranspiration were obtained at the Phillips Creek site for the 11 day period beginning on 27 August and ending 7 September 1989 (Julian dates 239–251) (Fig. 3). The value of observed head, 22 cm, corresponds to fully saturated conditions in the sediment with the water table at the sediment surface. The site of the tensiometer and net radiation measurements was flooded by high tides at least once every day, except Day 245. There was no rainfall at the site during this period.

Observed hydraulic head decreased during periods of evapotranspiration, reflecting the loss of water from storage in the sediment, and increased when storage was replenished by infiltration during tidal flooding. Observed head rose sharply to a peak when the wetland was flooded, and recession of flood waters was accompanied by a sharp drop in observed head. This response of head to flooding is caused by hydrostatic loading of the sediment by flood water as well as a change in water storage in the sediment (Hemond et al., 1984).

3.1. Choice of best model for changes in observed head

In the first stage of data analysis, we divided the record of observed head into 54 discrete time periods based on whether or not the marsh flooded and whether or not evapotranspiration occurred (Fig. 3). The periods when the marsh flooded were excluded from further consideration for the reasons discussed above. Measurements of head and temperature and the estimated evapotranspiration for the remaining 37 non-flooding periods provided the data used in the regression analysis (Table 3).

The best water balance model for non-flooding periods includes evapotranspiration and a constant inflow from the aquifer (Model 2a); this model had a residual mean square error of 26.2 cm^2 (the lowest of all of the models) (Table 4). The model explained 74% of the total variance in the raw Δh^* data (102 cm^2). Temperature had no significant residual effect on observed head; the estimated value for the parameter C_5 was not significantly different from zero. The regression coefficients associated with evapotranspiration, C_1, and constant groundwater inflow, C_2 and C_3, were significantly different from zero, and their values did not vary much between the different models examined. In contrast, the coefficient associated with the effect of hydraulic head in the sediment groundwater flow, C_4, was not significantly different from zero.

3.2. Variation of hydraulic properties

In the second stage of data analysis, we investigated the effect of hydraulic head (i.e. water content) on the hydraulic properties of the sediment and groundwater flux. The parameters in the selected water balance model (Model 2a, Table 2) were estimated as above but using subsets of the data defined by four equal intervals of mean head spanning the observed range of head. The results are summarized in Table 5, in terms of both the regression coefficients, C_1 and C_2, and the related parameters of the water

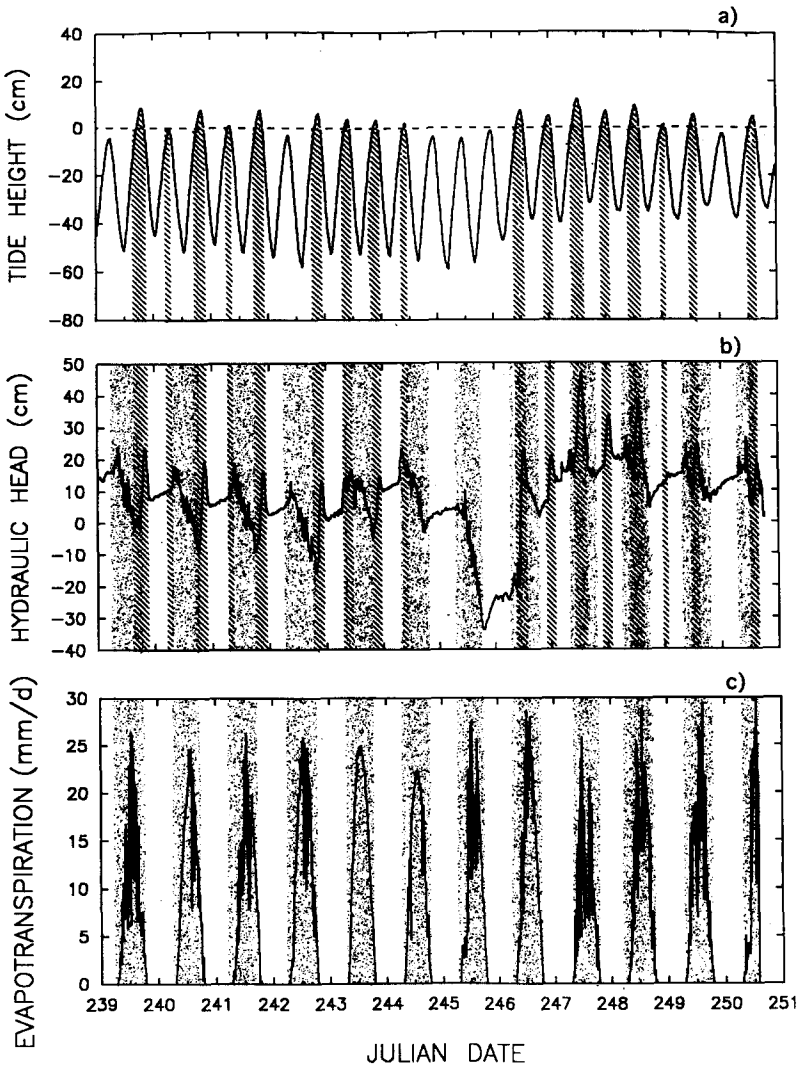

Fig. 3. Summary of water balance data recorded at the study site. Tide height is referenced to the elevation of the marsh surface; flooding occurs when tide height exceeds zero. Hydraulic head in the sediment is measured relative to an arbitrary datum. Evapotranspiration is calculated from measurements of net radiation. The period of data collection was partitioned into flooding periods (shown as hatched in graph (a)), non-flooding daytime periods with evapotranspiration (shown as shaded in graph (c)), and non-flooding night-time periods without evapotranspiration (shown as unhatched and unshaded in graph (b)) for the regression analysis. (Note that not all of the periods can be shown, owing to the scale of the figure.)

Table 3
Data used to estimate water balance parameters

Julian[1] day	Δt^2 (day)	$\bar{h}$ (cm)	Δh^* (cm)	EVAP (mm)	TEMP (°C)	ΔTEMP (°C)
239.000	0.292	14.4	2.6	0.0	−3.5	−1.3
239.292	0.451	6.2	−19.1	4.8	1.1	4.5
239.924	0.382	8.2	3.9	0.0	−2.0	−1.3
240.306	0.479	1.2	−17.8	6.1	2.3	4.0
240.951	0.340	6.0	3.6	0.0	−0.8	−0.9
241.292	0.035	7.5	−0.6	0.0	−0.8	0.3
241.410	0.382	1.6	−18.6	4.9	4.3	1.4
241.792	0.028	−7.4	0.6	0.0	3.3	−0.6
241.979	0.313	2.9	3.1	0.0	0.9	−0.5
242.292	0.507	−5.0	−18.9	6.6	3.8	3.4
242.799	0.056	−13.5	1.7	0.0	1.7	−3.8
243.007	0.278	2.3	4.3	0.0	−3.9	−1.6
243.319	0.063	10.6	−3.4	0.3	−1.2	2.7
243.507	0.292	−0.1	−6.4	4.8	1.8	−1.3
243.799	0.090	−1.3	4.0	0.0	−3.2	−5.6
244.007	0.299	12.3	7.5	0.0	−5.6	3.9
244.306	0.132	15.2	−1.8	0.8	0.3	3.4
244.514	0.278	4.0	−10.6	4.0	2.8	−0.3
244.792	0.521	0.7	3.9	0.0	0.3	−1.3
245.313	0.479	−16.3	−37.9	5.6	3.0	1.0
245.792	0.521	−28.5	13.3	0.0	−3.3	−7.3
246.313	0.132	−21.4	0.9	0.7	−3.6	4.1
246.618	0.174	4.6	−7.7	2.1	−1.3	−2.7
246.792	0.160	3.1	4.8	0.0	−3.9	−0.9
247.111	0.201	13.9	2.1	0.0	−5.8	2.7
247.313	0.139	17.6	5.3	0.7	−2.0	2.6
247.667	0.118	17.7	−8.5	0.8	−2.4	−1.8
247.785	0.181	15.0	3.2	0.0	−3.2	0.1
248.132	0.160	19.1	0.0	0.0	−3.9	−0.2
248.292	0.181	15.5	−7.2	1.5	−1.9	3.1
248.667	0.132	10.2	−7.3	0.8	−1.4	−2.3
248.799	0.243	9.3	5.4	0.0	−3.0	−0.3
249.125	0.181	13.7	0.6	0.0	−3.1	−0.3
249.306	0.208	10.7	−6.8	1.9	−1.7	1.5
249.590	0.201	14.5	−16.7	2.1	−1.9	−2.3
249.792	0.514	10.7	9.0	0.0	−7.0	−3.5
250.306	0.208	9.8	−10.8	1.8	−3.5	6.4

[1] Time at the beginning of period. Flooded periods are omitted.
[2] Length of each period.

balance. The smaller number of data points that fell in the two lower head ranges (Table 5) increased the uncertainty in estimating coefficient values, and as a result statistically significant values for the coefficients could not be determined for the head range −10 cm to 0 cm.

As expected, the hydraulic properties of the sediment changed as water content (mean head) varied. The specific yield increased 60% as the hydraulic head decreased

Table 4
Results of regression analysis

Models without temperature effect

Coefficient	Model 1a	Model 2a	Model 3a
C_1	−3.68 (0.39)[1]	−4.76 (0.47)	−4.77 (0.48)
C_2	–	13.3 (3.9)	–
C_3	–	–	13.4 (4.0)
C_4	–	–	0.05[2] (0.24)
Residual			
Mean square error	33.9	26.2	26.9[3]

Models with temperature effect

Coefficient	Model 1b	Model 2b	Model 3b
C_1	−3.39 (0.38)	−4.60 (0.52)	−4.58 (0.54)
C_2	–	12.7 (4.1)	–
C_3	–	–	12.6 (4.3)
C_4	–	–	−0.03[2] (0.27)
C_5	0.033[2] (0.02)	0.011[2] (0.02)	0.012[2] (0.02)
Residual			
Mean square error	32.1	26.7	27.5[2]

[1] Standard error of coefficient estimate.
[2] Regression coefficient not significantly different from zero.
[3] Residual mean square error is the sum of the squared residuals divided by the degrees of freedom, which decreases as the number of model parameters increases. Going from Model 2a to Model 3a, the residual mean square error increases even though the sum of the squared residuals decreases (better fit between model and data) because the degrees of freedom decreases from 35 (Model 2a) to 34 (Model 3a). The same occurs for Models 2b and 3b.

from the range 10–20 cm down to the range 0–10 cm, then decreased as head decreased further to the range −20 to −10 cm. This pattern of change in the specific yield of salt marsh sediment with decreasing head (water content) was also observed by Nuttle (1988). Slightly higher values of vertical groundwater inflow were estimated at lower ambient hydraulic heads. This was consistent with expectations based on Eq. (2), but the differences in the estimates of groundwater discharge were not significant. Therefore, the choice of water balance model in the initial analysis was not affected by these results.

3.3. Error analysis

Further refinement in the water balance model was not possible with the data collected because the residual error (the difference between observations and fitted model) was almost entirely accounted for by the random error in observed head. The standard error in observed head measured with one tensiometer is 5 cm, based on our calibration of the tensiometers. When measurements from two instruments are averaged, as we have done here to obtain the observed head data, the standard

Table 5
Effect of hydraulic head on regression coefficients

Head range (cm)	No. of points	Regression coefficients		Water balance parameter	
		C_1 (cm mm^{-1})	C_2 (cm day^{-1})	q_v[1] (mm day^{-1})	S_y[2] (cm cm^{-1})
$10 < h < 20$	15	−7.36	16.0	2.17	0.014
		(1.16)[3]	(4.79)	(0.65)	(0.01–0.02)[4]
$0 < h < 10$	14	−4.27	10.3	2.42	0.023
		(0.37)	(3.10)	(0.73)	(0.02–0.03)
$-10 < h < 0$	4	−2.20	−1.74	–[5]	–[5]
		(3.24)	(44.7)		
$-20 < h < -10$	4	−9.00	26.6	2.96	0.011
		(0.68)	(5.32)	(0.59)	(0.010–0.013)

[1] $q_v = -C_2/C_1$.
[2] $S_y = -1/C_1$.
[3] Standard error of coefficient estimate.
[4] 95% confidence interval.
[5] Regression coefficient not significantly different from zero.

error is reduced to 3.5 cm, assuming that the errors affecting one instrument are independent of the errors affecting the other instrument. Differencing the averaged observed heads to calculate Δh^* increases the standard error to 5 cm; this should be compared with the residual error for Model 2a of 5.1 cm (residual mean square error of 26.2 cm^2). If the errors in the instruments are correlated with each other, then averaging the two measurements does not reduce the expected mean square error. In the worst case, the error in the differenced, observed head is 7 cm, rather than 5 cm.

3.4. Cumulative sediment water balance

Groundwater accounted for 62% of the water removed from the sediment by evapotranspiration during the 11 day study; the remainder was supplied by infiltration and a small net decrease in water storage in the sediment (Fig. 1 and Table 6). Evapotranspiration totalled 60 mm for the entire period, of which we assume that only the 50 mm that occurred during non-flooded periods was removed from the sediment. The upward flux of groundwater q_v, was calculated from the ratio $-C_2/C_1 = 2.8$ mmday^{-1} (approximately 1 mm day^{-1} standard error), which translates to 31 mm (11 mm standard error) for the period. The net change in head between the beginning and the end of the period was −11 cm (7 cm standard error of measurement), which when multiplied by the storage coefficient, $-1/C_1 \approx 0.02$ cm cm^{-1}, yields a −2.2 mm change in water stored in the sediment. Infiltration for the period is obtained by difference, approximately 17 mm.

In the analysis presented above, the estimated evapotranspiration flux is the gage by which all other fluxes in the water balance are measured. The error in the estimated cumulative evapotranspiration translates directly into errors of the same relative magnitude in each of the fluxes estimated above. We estimate that this error may

Table 6
Cumulative water balance for 27 August–7 September

Length of record (days)	11.11
Net change in head (cm)	−11
Water fluxes (mm):	
Evapotranspiration[1]	−50
Infiltration[2]	17
Groundwater[3]	31 (11)[4]
Storage change[5]	2.2 (0.1)

[1] Wet potential evapotranspiration during non-flooding periods.
[2] Estimated by difference.
[3] Based on estimated groundwater flux rate; $q_v = -C_2/C_1$.
[4] Standard error of estimate.
[5] Based on change in head and storage coefficient, $S_y = 0.02\,\mathrm{cm\,cm^{-1}}$.

be as high as 20% (±10 mm for evapotranspiration over 11 days), based on errors in the sensors for direct measurement of net radiation (Field et al., 1992). A bias in evapotranspiration does not affect the relative magnitudes of the components of the water balance.

4. Discussion

Estimating the water balance in soils and sediments poses a difficult challenge. One is able to measure water fluxes in the soil only indirectly, and small variations in antecedent water content can have large effects on the magnitude of infiltration and evapotranspiration fluxes. Therefore the sources of error inherent in the estimation of water fluxes through soils merit close attention.

Our estimate of groundwater inflow is essentially the product of an estimated specific yield and the rate of rise of observed hydraulic head in the sediment at night, when there are no other fluxes of water into the sediment. An alternative approach would be to calculate this flux as the product of an estimated hydraulic conductivity and a measured gradient in head. We suggest that the specific yield of soils and sediments can be estimated with more accuracy than can their in-situ hydraulic conductivity. Although our measurements of short-term head fluctuations with the pressure transducer tensiometers suffered from relatively large errors, the rate of rise of head owing to groundwater could be determined with a reasonable degree of precision.

4.1. Groundwater flow estimated using hydraulic conductivity

It is useful to compare the estimated groundwater inflow obtained here with results obtained by the gradient-based method. Chambers et al. (1992) estimated groundwater inflow near our site, for roughly the same period of time, based on in-situ estimates of hydraulic conductivity of the sediment and the vertical gradient in hydraulic head. Their estimated flux rate is two orders of magnitude smaller than

ours. We cannot account for the discrepancy between the two estimates; however, we note that, in general, gradient-based estimates of water fluxes in soils are affected by uncertainties in the estimated in-situ hydraulic conductivity, especially where the hydraulic conductivity is low and the material exhibits a great deal of spatial variability, including the possibility of preferred pathways for flow.

Other considerations raise questions about the straightforward application of Darcy's law to estimate groundwater discharge into intertidal wetland sediments. First, osmotic potential can play a role in driving the flow of fresh water from one geologic stratum into another containing saline water (Freeze and Cherry, 1979, p. 104). In the case of fresh groundwater discharging into sediments with porewater salinities comparable with seawater, the difference in osmotic 'head' is on the order of 10^4 cm, which is much higher than differences in hydraulic head measured between piezometers in the sediment and the Wachapreague formation at our site. Second, water can move between vertical layers of sediment through living plant roots. This movement occurs in addition to uptake and transpiration by the above-ground portion of the plants (Richards and Caldwell, 1987). In effect, living roots can increase the vertical hydraulic conductivity of the soil. Neither of these phenomena was considered in the flux calculation by Chambers et al.

These comments do not resolve the difference in results obtained by us and Chambers et al. That would require a side-by-side comparison in a field test and further exploration of the issues raised above. However, our approach appears to be subject to less error.

4.2. Implications for the solute balance

Groundwater inflow was not sufficient to prevent a net advection of salt into the sediment during the period of study. As long as groundwater inflow is less than evapotranspiration salt will continue to be carried into the sediment during tidal flooding, and the problem of salt accumulation remains. Under these conditions, salt can be removed across the sediment surface only by diffusion, during flooding, and by uptake and translocation by vegetation.

Our estimated rate of groundwater inflow is approximately of the same magnitude as the average annual evaporation rate for our site (Kohler et al., 1959). We speculate that, as evapotranspiration exceeded groundwater flow by only 1.5 mm day^{-1} in late summer, the inflow of groundwater may well exceed evapotranspiration at other times of the year. If this were to occur, then the sediment will be held at full saturation as the inflow of groundwater from below drives seepage from the sediment surface. Groundwater flow in excess of evapotranspiration will prevent infiltration of brackish water during tidal flooding and flush salt and other solutes out of the sediment. The possibility of seasonal purging of solutes from the sediments of intertidal wetlands merits further attention.

Acknowledgments

We are grateful to Rob Hoelscher for his assistance in assembling, calibrating and

maintaining the pressure transducer tensiometers. This work was funded in part by NSF Grant BSR-8702333 to the Virginia Coast Reserve LTER program at the University of Virginia.

Appendix: systematic error in observed head

The pressure transducers used in the tensiometers produce an output voltage as a linear function of the pressure applied to the transducer. Under field conditions the output voltage of the assembled tensiometers was also affected by ambient temperature even though, according to manufacturer's specifications, the pressure transducers were temperature compensated. By calibration under field conditions we were able to remove a temperature-related offset in the output voltage, i.e. temperature drift, by subtracting the output of a reference tensiometer from the outputs of the two tensiometers measuring head in the sediment (Hoelscher et al., 1993). The reference tensiometer was held at constant hydraulic head. This tensiometer was identical to the two active tensiometers in construction and subjected to the same temperature conditions. After correcting for temperature drift, the estimated standard deviation of the total error in observed head was 5 cm, still relatively large compared with the magnitude of fluctuations in head in the sediment that we expected would occur over the course of a day. Therefore, it was necessary to account for measurement error in interpreting changes in observed head. In particular, we anticipated that the error in observed head may include a residual component of systematic error related to temperature. Here, we derive an expression for this error.

The following equation describes the output voltage of the tensiometers as a linear function of actual head (i.e. pore pressure) in the sediment and ambient temperature (i.e. temperature of the instrumentation).

$$v = A(\theta - \theta_r)(h - h_r) + B(h - h_r) + C(\theta - \theta_r) + v_r \tag{A1}$$

where v is output voltage, v_r is a reference voltage, h is hydraulic head, h_r is a reference head, θ is ambient temperature, θ_r is a reference temperature, and A, B, and C are constants. In this equation, output voltage is a linear function of head, when temperature is constant, and a linear function of temperature, when head is constant. The first term on the right-hand side of Eq. (A1) can be interpreted as the effect of temperature on the sensitivity of the output voltage to differences in head. The term $C(\theta - \theta_r)$ is the temperature-related drift in output, which was detected and corrected for in our calibration. In analyzing the observed head data we are primarily interested in knowing whether a residual systematic error related to temperature exists that is large enough to affect the estimates of the components of the water balance. A linear approximation to the relationship between observed head and temperature is sufficient for estimating the error term as long as the relationship is monotonic but not necessarily linear.

Solving Eq. (A1) for head,

$$h = h_r + \frac{v - v_r}{B} - \frac{C}{B}(\theta - \theta_r) - \frac{A}{B}(\theta - \theta_r)(h - h_r) + \epsilon_r \tag{A2}$$

in which the first three terms on the right-hand side can be evaluated based on our calibration of the instruments. Therefore in this study, observed head, h^*, is defined as

$$h^* \equiv h_r + \frac{v - v_r}{B} - \frac{C}{B}(\theta - \theta_r) = h + \frac{A}{B}(\theta - \theta_r)(h - h_r) + \epsilon_r \tag{A3}$$

from which it can be seen, with reference to Eq. (3), that the remaining systematic error in observed head has the form

$$\epsilon_s = \frac{A}{B}(\theta - \theta_r)(h - h_r) \tag{A4}$$

References

Capone, G. and Slater, J.M., 1990. Interannual patterns of watertable height and groundwater derived nitrate in near-shore sediments. Biogeochemistry, 10: 277–288.

Chambers, R.M., Harvey, J.W. and Odum, W.E., 1992. Ammonium and phosphate dynamics in a Virginia salt marsh. Estuaries, 15: 349–359.

Draper, N.R. and Smith, H., 1981. Applied Regression Analysis. Wiley, New York, 709 pp.

Fetsko, M.E., 1990. A Water Balance Estimate at Brownsville, Virginia. M.Sc. Thesis, Department of Environmental Sciences, University of Virginia, Charlottesville.

Field, R.T., Fritschen, L., Kanemasu, E.T., Smith, E.A., Stewart, J., Verma, S. and Kustas, W., 1992. Calibration, comparison, and correction of net radiation instruments used during FIFE. J. Geophys. Res., 97(017): 18681–18695.

Freeze, R.A. and Cherry, J.A., 1979. Groundwater. Prentice–Hall, Englewood Cliffs, NJ.

Harvey, J.W. and Nuttle, W.K., 1995. Fluxes of water and solute in a coastal wetland sediment. 2. Effect of macropores on solute exchange with surface water. J. Hydrol., 164: 109–125.

Harvey, J.W. and Odum, W.E., 1990. The influence of tidal marshes on upland groundwater discharge to estuaries. Biogeochemistry, 10: 217–236.

Harvey, J.W., Germann, P.F. and Odum, W.E., 1987. Geomorphological control of subsurface hydrology in the creekbank zone of tidal marshes. Estuarine Coastal Shelf Sci., 25: 677–691.

Hemond, H.F., Nuttle, W.K., Burke, R.W. and Stolzenbach, K.D., 1984. Surface infiltration in salt marshes: theory, measurement, and biogeochemical implications. Water Resour. Res., 20: 591–600.

Hoelscher, J.R., Nuttle, W.K. and Harvey, J.W., 1993. The calibration and use of pressure transducers in tensiometer systems. Hydrol. Processes, 7: 205–211.

Johannes, R.E., 1980. The ecological significance of the submarine discharge of groundwater. Mar. Ecol. Prog. Ser., 3: 365–373.

Johannes, R.E. and Hearn, C.J., 1985. The effect of groundwater discharge on nutrient and salinity regimes in a coastal lagoon of Perth, Western Australia. Estuarine Coastal Shelf Sci., 21: 789–800.

Keidser, A. and Rosbjerg, D., 1991. A comparison of four inverse approaches to groundwater flow and transport parameter identification. Water Resour. Res., 27: 2219–2232.

Kohler, M.A., Nordenson, T.J. and Baker, D.R., 1959. Evaporation maps for the United States. Technical Paper 37, US Weather Bureau, Department of Commerce, Washington, DC.

Mixon, R.B., 1985. Stratigraphic and geomorphic framework of uppermost Cenozoic deposits in the southern Delmarva peninsula, Virginia and Maryland. US Geol. Surv. Prof. Pap. 1067-G.

Morris, J.T., Kjerfve, B. and Dean, J.M., 1990. Dependence of estuarine productivity on anomalies in mean sea level. Limnol. Oceanogr., 35: 926–930.

Nuttle, W.K., 1988. The interpretation of transient pore pressures in salt marsh sediment. Soil Sci., 146: 391–402.

Nuttle, W.K. and Hemond, H.F., 1988. Salt marsh hydrology: implications for biogeochemical fluxes to the atmosphere and estuaries. Global Biogeochem. Cycles, 2: 91–114.

Price, J.S. and Woo, M.K., 1988. Studies of a sub-arctic coastal marsh: I. Hydrology. J. Hydrol., 103: 275–292.

Priestly, C.H.B. and Taylor, R.J., 1972. On the assessment of surface heat flux and evaporation using large-scale parameters. Mon. Weather Rev., 100: 81–92.

Reilly, T.E. and Goodman, A.S., 1985. Quantitative analysis of saltwater–freshwater relationships in groundwater systems—a historical perspective. J. Hydrol., 80: 125–160.

Richards, J.H. and Caldwell, M.M., 1987. Hydraulic lift: substantial water transport between soil layers by *Artemisia tridentata* roots. Oecologia, 73: 486–489.

Schuh, W.M., Klinkebiel, D.L. and Gardner, J.C., 1993a. Use of an integrated transient flow and water budget procedure to predict and partition components of local recharge. J. Hydrol., 148: 27–60.

Schuh, W.M., Meyer, R.F., Sweeney, M.D. and Gardner, J.C., 1993b. Spatial variation of root-zone and shallow vadose-zone drainage on a loamy glacial till in a sub-humid climate. J. Hydrol., 148: 1–26.

Statistical Analysis Systems Institute, Inc., 1989. SAS/STAT Users Guide, Version 6, 4th edn, Vol. 2. SAS Institute. Inc., Cary, NC, 846 pp.

Yeh, W.W-G., 1986. Review of parameter identification procedures in groundwater hydrology: the inverse problem. Water Resourc. Res., 22: 95–108.

Yelverton, G.F. and Hackney, C.W., 1986. Flux of dissolved organic carbon and pore water through the substrate of a *Spartina alterniflora* marsh in North Carolina. Estuarine Coastal Shelf Sci., 22: 255–267.